Nat. Hazards Earth Syst. Sci., 14, 2313–2320, 2014
www.nat-hazards-earth-syst-sci.net/14/2313/2014/
doi:10.5194/nhess-14-2313-2014

Natural Hazards and Earth System Sciences
Open Access

Development of models for maximum and time variation of storm surges at the Tanshui estuary

C.-P. Tsai[1] **and C.-Y. You**[2]

[1]Department of Civil Engineering, National Chung Hsing University, Taichung 402, Taiwan
[2]Water Resource Bureau, Taichung City Government, Taichung 420, Taiwan

Correspondence to: C.-P. Tsai (cptsai@dragon.nchu.edu.tw)

Received: 16 October 2013 – Published in Nat. Hazards Earth Syst. Sci. Discuss.: 10 December 2013
Revised: 18 July 2014 – Accepted: 27 July 2014 – Published: 1 September 2014

Abstract. In this study, artificial neural networks, including both multilayer perception and the radial basis function neural networks, are applied for modeling and forecasting the maximum and time variation of storm surges at the Tanshui estuary in Taiwan. The physical parameters, including both the local atmospheric pressure and the wind field factors, for finding the maximum storm surges, are first investigated based on the training of neural networks. Then neural network models for forecasting the time series of storm surges are accordingly developed using the major meteorological parameters with time variations. The time series of storm surges for six typhoons were used for training and testing the models, and data for three typhoons were used for model forecasting. The results show that both neural network models perform very well for the forecasting of the time variation of storm surges.

1 Introduction

A storm surge is a meteorological tide characterized by an abnormal rise in level of sea water, primarily induced by the low atmospheric pressures associated with a tropical storm, usually typhoons in the case of Taiwan, which is located on the western side of the Pacific Ocean. The height of a storm surge at a particular location is expressed as the value obtained by subtracting the predicted astronomical tide from the actual recorded sea level (Horikawa, 1978). The risk of flooding in low-lying coastal areas increased with the combination of higher spring tides along with serious storm surges.

The simplest method for forecasting the maximum storm surge is to use an empirical formula (Conner et al., 1957; Horikawa, 1978). Generally, storm surges have been predicted using numerical methods. For example, Kawahara et al. (1980), Westerink et al. (1992), Blainetal (1994), and Hsu et al. (1999) applied the finite element method for this purpose, while Yen and Chou (1979), Walton and Christensen (1980), Harper and Sobey (1983), and Hwang and Yao (1987) applied the finite difference method with nonlinear shallow water equations to simulate storm surges. Coupled wave-surge models have been proposed to simulate coastal flooding resulting from storm surges and waves generated by tropical cyclones (Cheung et al., 2003). Recently, Doong et al. (2012) developed an operational coastal flooding early warning system that considered both wave setup and storm surge, in which the storm surge is predicted by the Princeton Ocean Model (POM). Xu et al. (2014) integrated Monte Carlo and hydrodynamic models for estimating extreme water levels that occurred as a consequence of a storm surge.

In recent years, with the maturing of neural network technology, it has been widely applied to the modeling of nonlinear natural phenomena. For example, Grubert (1995) used feed-forward back-propagation neural networks to predict the flow rate at a river mouth. Deo and Sridhar Naidu (1999) used neural networks to build a model for real-time wave prediction. The results show that neural network models perform better than autoregressive models for wave prediction. Tsai and Lee (1999) used a back-propagation neural network for real-time tide prediction. Tsai et al. (2002) used the back-propagation neural network for forecasting and supplementing the time series of wave data using neighboring stations'

wave records. Lee et al. (2002) used short term observation data to predict long-term tidal levels with a back-propagation neural network. Sztobryn (2003) used neural networks to predict storm surges and compared the results obtained using different neural network topologies.

Tsai et al. (2005) used a back-propagation neural network for the training of a sea level time series model using data from previous typhoons as the training data from which to predict later typhoons. However, the model was only used to predict sea levels during storms, rather than the storm surge. In practice, astronomical tides plus storm surges combine to increase sea levels during storms. Currently, astronomical tides can be accurately predicted using harmonic analysis or numerical methods. Moreover, the combination of maximum storm surge plus high spring tides should be considered in the analysis of possible risk of coastal inundation. Thus, the first part of this study is aimed at the development of neural network models for estimating the maximum storm surge. The results trained by the neural networks are compared with the empirical formula proposed by Horikawa (1978).

Tseng et al. (2007) developed a back-propagation neural network model for predicting the time variation of storm surges. They suggested a total 18 factors as the inputs, including the astronomical tidal level. However, this seems to violate the physical definition of a storm surge as caused by abnormal meteorological conditions and is not dependent on the astronomical tide. A training process of a neural network enables the neural system to capture the complex and non-linear relationships between the known input data and the desired output data (Lin and Chen, 2006). Thus the selection of the appropriate input parameters in the neural network is necessary; especially the parameters between the input and output should be taken into consideration with some physical relationships. Accordingly, differing from Tseng et al. (2007), the second part of this study proposed the neural network models, including both multilayer perception and the radial basis function neural networks, for forecasting the time variation of storm surges using a very few appropriate major meteorological factors based on the first part of the current study. The performance of the present model is assessed by the agreement indices including the correlation coefficient and root-mean-square error between the observed and forecasted results.

2 Neural networks

The artificial neural network is an information-processing system which mimics the biological neural networks of the human brain by interconnecting many artificial neurons. There are many types of the neural networks, but the multilayer perception (MLP) network and the radial basis function (RBF) network are adopted in this study. The theory of neural networks is discussed in detail in Haykin (1999).

2.1 Multilayer perception network

An MLP network is a supervised learning technique with a topology that contains one input layer, one or more hidden layers, and one output layer. An MLP network with one hidden layer is adopted in this study. Data are sent to the output layer from the input layer using the feed-forward method formulated as follows:

$$y_j = f(\mathrm{net}_j) \tag{1}$$

$$\mathrm{net}_j = \sum_{i=1}^{N} W_{ij} X_i - B_j, \tag{2}$$

where y_j is the output variable, W_{ij} is the weight between the jth neuron and the ith neuron, X_i is the input variable that acts as a biomimetic neuron input signal, $f(\mathrm{net}_j)$ is the transformation function that acts as a biomimetic non-linear function of the neurons, B_j is the threshold (bias) for the jth neuron, and net_j is the consolidation function for the jth neuron.

An activation function – usually an S-curve called a sigmoid function – is included, which increases stability and can be written as

$$y_j = f(\mathrm{net}_j) = (1 + e^{-\mathrm{net}_j})^{-1}. \tag{3}$$

The main procedure in MLP network learning is the backward propagation of the error estimated at the output layer to the input layer through the hidden network layer to obtain the final desired outputs. The gradient descent method is utilized in this study to calculate the weight of the network and to adjust the weight of the interconnections for minimizing the output error. The algorithm is discussed in detail in Rumelhart et al. (1986).

2.2 Radial basis function network

The topology of the radial basis function (RBF) network is similar to that of the MLP network. Basically, the most advantageous feature of the RBF network is its fast learning speed, meaning it can be applied to real-time systems. Its output can be written as follows:

$$F(\boldsymbol{x}') = \sum_{j=1}^{N} w_j \varphi_j(\boldsymbol{x}') + B_j, \tag{4}$$

where $\boldsymbol{x}'$ is the input vector, w_j is the weight from the jth neuron to the output neuron, B_j is the threshold (bias) for the jth neuron, φ_j is the basis function of the jth layer, and $F(\boldsymbol{x}')$ is the output function of the network. The transfer function for the neurons in the output layer is a linear function.

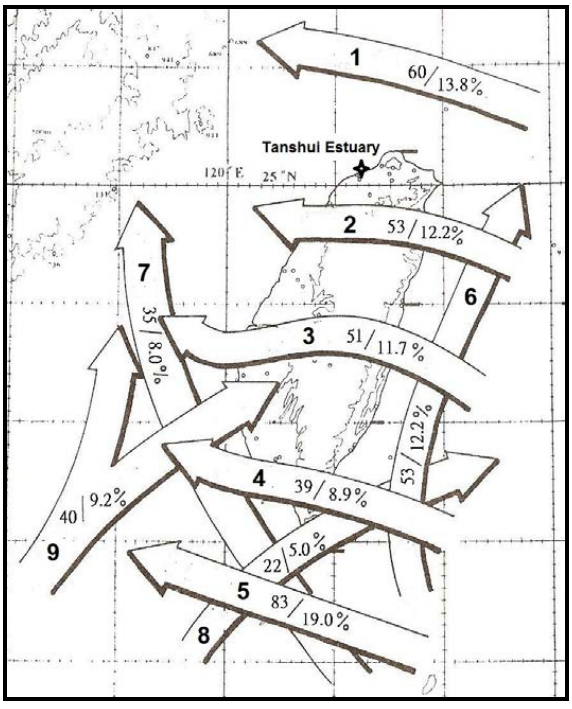

Figure 1. Categories of typhoon tracks affecting Taiwan from 1897 to 2007 (Central Weather Bureau, Taiwan).

Table 1. Observed data of the maximum storm surges.

Nos.	Typhoons	ζ_{max} (m)	V_{max} ($m\,s^{-1}$)	ΔP (mb)	$\cos\theta$
1	Longwang	0.135	8.1	16.55	−0.00175
2	Talim	0.369	8.9	39.25	−0.64279
3	Haitane	0.294	8.1	38.55	−0.00175
4	Matsa	0.561	8.6	26.55	−0.98481
5	Lekima	0.305	5.3	20.65	0.50000
6	Nari	0.220	7.1	16.15	0.76604
7	Toraji	0.165	5.1	20.15	−0.34202
8	Chebi	0.227	7.1	19.35	−0.76604
9	Xangsane	0.881	9.1	14.55	0.98481
10	Bilis	0.290	8.8	24.75	−0.64279
11	Prapiroon	0.588	5.2	22.95	0.50000
12	Kaitai	0.425	6.7	28.25	0.34202
13	Dan	0.435	7.1	12.65	−0.34202
14	Babs	0.247	3.6	7.15	0.92388
15	Zeb	0.799	11.7	30.75	0.70711
16	Yanni	0.183	5.4	15.25	1.00000
17	Otto	0.191	6.3	18.65	−0.70711
18	Ivan	0.523	2.8	8.75	0.70711
19	Amber	0.240	7.6	24.65	−0.70711
20	Winnie	0.925	11.7	32.85	0.00000
21	Herb	0.953	9.9	47.75	1.00000
22	Gloria	0.201	7.6	25.65	−0.70711

A common basis function used for the RBF network is the Gaussian function, which can be written as follows:

$$\varphi_j(\boldsymbol{x}') = \exp\left(-\frac{\left\|\boldsymbol{x}' - u_j\right\|^2}{2\sigma_j^2}\right), \quad j = 1, 2, 3 \ldots N, \tag{5}$$

where σ_j is the smoothing parameter of the jth neuron which controls the radial basis function, u_j is the center of the neurons in the jth radial basis function in the hidden layer, and $\left\|\boldsymbol{x}' - u_j\right\|$ is the Euclidean distance between u_j and the input vector.

3 Data sources

According to Murty (1984), over the past century, an average of 3.5 typhoons per year have struck Taiwan. Storm surges as a consequence of these events are very likely to occur in the northern areas of Taiwan such as the Tanshui estuary located on the edge of the Taiwan Strait. Thus, this study collected data from the station at the Tanshui estuary which was then used in our exploration of forecasting models for storm surges. Data on storm surges and weather during typhoons that occurred between 1996 and 2001 and in 2005 were acquired from this station. The Central Weather Bureau (CWB) of Taiwan has categorized typhoons from 1897 to 2007 into nine subgroups based on the tracks they follow across Taiwan; see Fig. 1. According to Tsai et al. (2000), the risk of storm surge at the Tanshui estuary is most likely for typhoons following the first, second and sixth tracking paths. A total of 22 storm events that impacted the Tanshui estuary were selected, and the observed data of the maximum storm surges were summarized in Table 1. Data on the flow rate were also collected from Xiulang station, about 25 km upstream station from the Tanshui estuary.

Before training a neural network, pre-processing of input data is necessary to fit the range of the activation function used in the network. The input data are normalized using the following equation:

$$x_{i_{new}} = \left[D_{min} + \frac{x_{i_{old}} - x_{min}}{x_{max} - x_{min}}\left(D_{max} - D_{min}\right)\right], \tag{6}$$

where D_{min} and D_{max} represent the range to be mapped, x_{max} and x_{min} are the maximum and minimum values of all data, and $x_{i_{old}}$ and $x_{i_{new}}$ are the values before and after transformation.

Generally, network performances can be efficiently evaluated by two agreement indices – the root-mean-square errors (RMSEs) and correlation coefficients (C.C.) – which are defined as follows:

$$\mathrm{RMSE} = \sqrt{\frac{\sum_{k=1}^{n}(y_k - \hat{y}_k)^2}{n}}, \tag{7}$$

Table 2. Comparison of the agreement indices of the maximum storm surges obtained with different models.

Models		$I_x H_y O_z$	Agreement indices		Input variables
Empirical formula		–	RMSE	0.267	$\Delta P, U$
			C.C.	0.565	
Model A	MLP	$I_1 H_7 O_1$	RMSE	0.156	ΔP
			C.C.	0.801	
Model A	RBF	$I_1 H_8 O_1$	RMSE	0.172	ΔP
			C.C.	0.752	
Model B	MLP	$I_2 H_7 O_1$	RMSE	0.048	$\Delta P, U$
			C.C.	0.983	
Model B	RBF	$I_2 H_{11} O_1$	RMSE	0.094	$\Delta P, U$
			C.C.	0.935	
Model C	MLP	$I_3 H_6 O_1$	RMSE	0.038	$\Delta P, U, Q$
			C.C.	0.985	
Model C	RBF	$I_3 H_{10} O_1$	RMSE	0.110	$\Delta P, U, Q$
			C.C.	0.906	

in which n is the number of samples, $\hat{y}_k$ is the value of the observations and y_k denotes the value of the predictions.

$$\text{C.C.} = \frac{\sum_{k=1}^{n} (y_k - \bar{y}) \left(\bar{\hat{y}} - \bar{y}\right)}{\sqrt{\sum_{k=1}^{n} (y_k - \bar{y})^2 \sum_{k=1}^{n} \left(\bar{\hat{y}} - \bar{y}\right)^2}}, \tag{8}$$

where $\bar{\hat{y}}$ is the average value of the observations, and $\bar{y}$ is the average of value of the predictions.

4 Models for maximum storm surge

4.1 Empirical formula

Studies of storm surges at specific spots are more meaningful with higher practical values. Thus the maximum storm surge plus the highest spring tide is used for analysis of the potential of coastal inundation. Conner et al. (1957) proposed that a larger center of low pressure would lead to the recording of a higher wind speed at a station and thus derived an empirical formula in terms of a single parameter, the pressure at the center of the storm, to forecast the value of the extreme storm surge.

Horikawa (1978) proposed that, in addition to pressure, the wind speed and wind direction should also be taken into consideration in the estimation of storm surges. Based upon observed data from Japan, they derived an empirical formula for forecasting the maximum storm surge which is given using

$$\zeta_{\max} = A\Delta P + BV_{\max}^2 \cos\theta, \tag{9}$$

where $\zeta_{\max}$ is the maximum storm surge, ΔP is the maximum pressure difference between the spatial mean pressure and the lowest atmospheric pressure on the sea surface during the storm, $V_{\max}$ is the maximum wind speed during the typhoon, θ is the angle between the direction of the wind with the maximum wind speed and the tide-gauge station normal line, and A and B are constants determined empirically from the observed data. Based on the 22 selected storm surges listed in Table 1, the empirical constants for the Tanshui estuary, obtained through regression analysis, are $A = 0.00952$ and $B = 0.0031$.

4.2 Estimations by neural networks

Based on the physical parameters used in previous empirical formulas, three models with different combined input variables for both MLP and RBF neural networks are investigated. In the first model, denoted Model A, as in Conner (1957) the maximum pressure difference is the only input variable considered in the estimation of the maximum storm surge. Subsequently, another input variable, the wind field factor, including the maximum wind speed and the corresponding wind direction, is added to produce Model B. Finally, in addition to the maximum pressure difference and the corresponding wind factor, the upstream flow rate is also input to produce Model C. The three models are expressed as

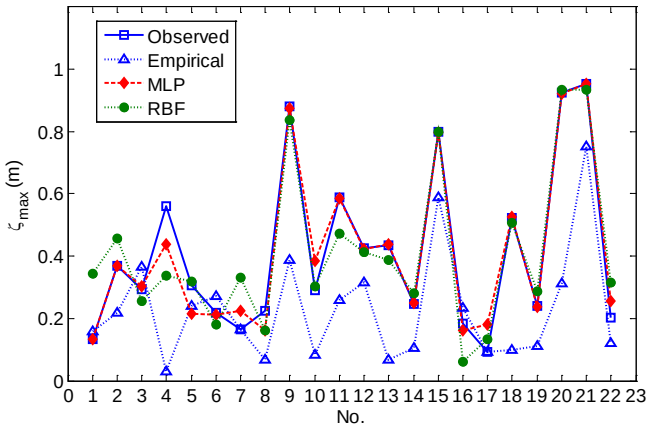

Figure 2. Comparison between the observed and estimated maximum storm surges obtained using MLP, RBF and the empirical formula.

follows:

$$\text{Model A}: \zeta_{\max} = f(\Delta P) \quad (10)$$

$$\text{Model B}: \zeta_{\max} = f(\Delta P, U) \quad (11)$$

$$\text{Model C}: \zeta_{\max} = f(\Delta P, U, Q), \quad (12)$$

where ΔP is the maximum pressure difference, $U = V_{\max}^2 \cos\theta$ is the wind field factor, and Q is the upstream flow rate.

The topologies of the neural networks are presented in the form of "$I_x H_y O_z$", where I_x represents the number of neurons in the input layer, H_y represents the number of neurons in the hidden layer, and O_z represents the number of neurons in the output layer. Thus, they are I_1, I_2, and I_3 of Models A, B and C, respectively, and the outputs of all models are O_1. The optimum number of neurons in the hidden layer is dependent on the complexities and nonlinearities of the problems and is generally obtained by trial and error. Note that 16 of the total 22 observed data shown in Table 1 are used for training the neural networks, and the other data are used for testing.

Table 2 shows the performance of Models A, B and C for both MLP and RBF neural networks, as well as the empirical formula by Horikawa (1978). It can be seen that the results from Model B are more precise than those from Model A. This implies that for accurate estimation of the storm surge one should not be too dependent on one single pressure variable, even though the wind speed depends on the pressure deficiency. It can also be seen that the performance of the neural networks is much better than that of the empirical formula, although the input variables used in Model B are the same as those used in Horikawa's formula (1978). This outcome shows that neural networks are suitable for modeling the nonlinear interrelationships among the physical parameters.

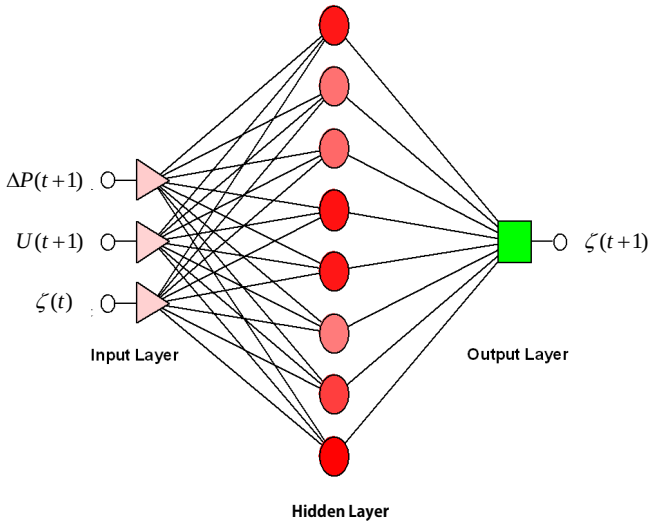

Figure 3. Sketch of the architecture of the neural network for forecasting the time variation of storm surges.

Table 3. Nine typhoon events used for training, test and forecasting the neural network models for the time variation of storm surges.

Typhoon tracks	Names	Intensity grades	Used for
First track	Herb (1996)	Severe	Training
	Haitane (2005)	Severe	Test
	Matsa (2005)	Severe	Forecast
Second track	Bilis (2000)	Severe	Test
	Lekima (2001)	Middle	Training
	Talim (2005)	Severe	Forecast
Sixth track	Zeb (1998)	Severe	Training
	Kaitai (2000)	Middle	Test
	Xangsane (2000)	Middle	Forecast

The object discussed in this study is the storm surge at an estuary, so the influence of the upstream flow is also investigated. According to the values of the agreement indices shown in Table 2, the performance of Model C is as good as Model B. This likely demonstrates that the influence of the upstream flow on the storm surge at the Tanshui estuary is far smaller than the influence of the wind field or atmospheric pressure.

Figure 2 shows a comparison of the observed and estimated maximum storm surges obtained for the MLP and RBF neural networks with Model B, as well as with the empirical formula by Horikawa (1978). The results of both the MLP and RBF neural networks are precise, especially for the larger storm surges; however, the estimations obtained using the empirical formula are mostly lower than the observed values.

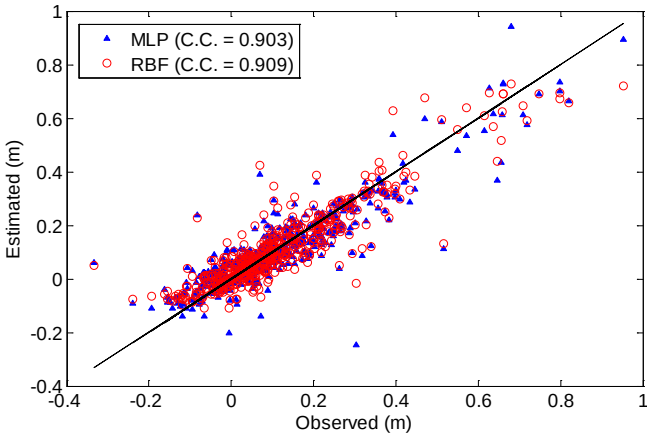

Figure 4. The scatterplot between observed data and trained/tested results from MLP and RBF neural networks.

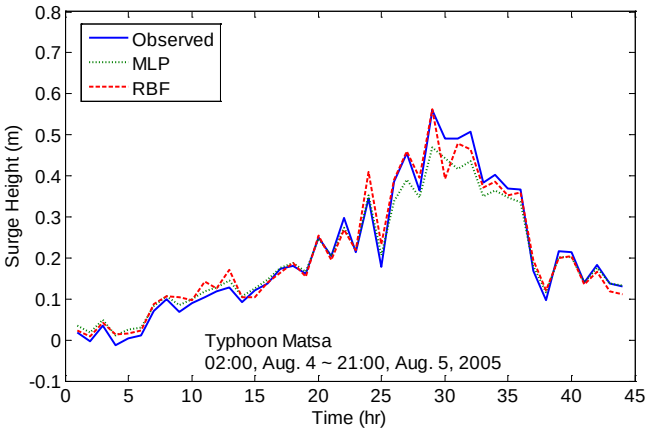

Figure 5. Comparison of the observed data and results forecast by the MLP and RBF neural networks for Typhoon Matsa.

5 Forecasting models for time series of storm surges

The major factors used in Model B with time variations can be applied to build the forecast models to estimate the time series of storm surges. The present neural networks are aimed at forecasting the storm surge at time $t+1$, that is, $\zeta(t+1)$. This is done by using the inputs including the pressure difference and wind factor at time $t+1$, $\Delta P(t+1)$ and $U(t+1)$, and the storm surge at the previous time t, $\zeta(t)$. This can be expressed as

$$\zeta(t+1) = f[\Delta P(t+1), U(t+1), \zeta(t)]. \quad (13)$$

The reason why $\zeta(t)$ is used as an input variable for the neural network models is because the storm surge at time t acts a reference value for the next time $t+1$. The architecture of the neural network is depicted in Fig. 3. Note that information about the pressure difference and wind field at time $t+1$ for a typhoon can be taken from the warning reports issued by the CWB; thus the time series of the storm surge can be consecutively forecast.

The time series of storm surges for nine typhoon events are selected, in which six of events are used for the model's training and testing, and the other three are used for forecasting, as shown in Table 3. The scatterplot for the correlation coefficients between observed data and trained/tested results of both MLP and RBF neural networks is depicted in Fig. 4, from which the high correlations are obtained. This indicates that both MLP and RBF neural networks are capable of forecasting the time variation of storm surges. It should be noted that the best topologies of the MLP and RBF models are $I_3H_8O_1$ and $I_3H_{10}O_1$, respectively.

Figures 5–7 show the forecast results by the trained neural networks for the time series of storm surges caused by Typhoon Matsa, Typhoon Xangsane, and Typhoon Talim, respectively. Two of these were categorized as severe typhoons, and one was a mid-strength typhoon. Table 4 lists the values of the agreement indices for the forecast results. It can be

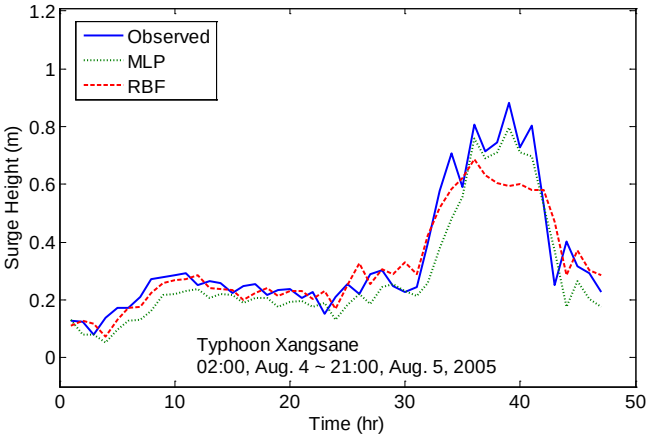

Figure 6. Comparison of the observed data and results forecast by the MLP and RBF neural networks for Typhoon Xangsane.

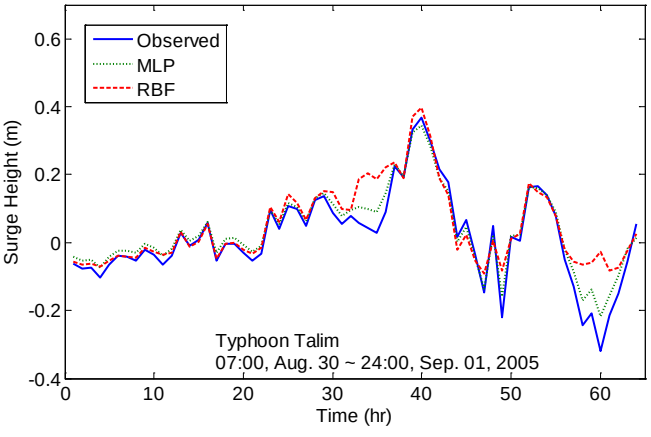

Figure 7. Comparison of the observed data and results forecast by the MLP and RBF neural networks for Typhoon Talim.

Table 4. The values of agreement indices of the forecast time series of storm surges.

Typhoon names	Models	Agreement indices	
Matsa	MLP	RMSE	0.074
		C.C.	0.886
	RBF	RMSE	0.077
		C.C.	0.866
Talim	MLP	RMSE	0.032
		C.C.	0.984
	RBF	RMSE	0.070
		C.C.	0.881
Xangsane	MLP	RMSE	0.118
		C.C.	0.924
	RBF	RMSE	0.090
		C.C.	0.919

seen that high correlation coefficients and low RMSEs between the forecast and observed data are obtained. Accordingly, the storm surges could be well forecast by the present neural network models using 3 major physical factors – local pressure, wind speed and direction – rather than using the complicated 18 input factors presented in Tseng et al. (2007).

6 Conclusions

Storm surges caused by meteorological factors are not easy to precisely forecast using empirical formulas. This study adopted the technology of MLP and RBF neural networks to build models for forecasting the variation of storm surges based on historic data. First, the optimum neural network models were trained and tested to estimate the maximum storm surges based on the major meteorological factors including the atmospheric pressure difference, wind speed and wind direction. Then these major factors with time variations were applied to build the forecast models to estimate the time series of storm surges. The estimation results for the maximum storm surges show that both the MLP and RBF neural network models are precise, especially for the larger storm surges. For the time variation of storm surges, the storm surge at time $t+1$ could be forecast well by neural networks based upon three major meteorological factors, including the local pressure, wind speed and direction at time $t+1$ and the surge height at previous time t.

Acknowledgements. The authors are appreciative of the support from the Ministry of Science and Technology, Taiwan, under grant no. NSC 96-2221-E-005-077-MY3. They are also most grateful for the constructive comments from J. W. de Vries and M. Bajo, all of which have led to several corrections and have greatly aided us in the improvement of the presentation of this paper. The authors also thank to C.-Y. Chen for his contribution.

Edited by: N. Pinardi
Reviewed by: J. W. de Vries and M. Bajo

References

Blainetal, C. A., Westerink, J. J., and Luettich Jr., R. A.: The influence of domain size on the response characteristics of a hurricane storm surge model, J. Geophys. Res., 99, 18467–18479, 1994.

Cheung, K. F., Phadke, A. C., Wei, Y., Rojas, R., Douyere, Y. J. M., Martino, C. D., Houston, S. H., Liu, P. L. F., Lynett, P. J., Dodd, N., Liao, S., and Nakazaki, E.: Modeling of storm-induced coastal flooding for emergency management, Ocean Eng., 30, 1353–1386, 2003.

Conner, W. C., Kraft, R. H., and Harris, L. D.: Empirical methods for forecasting the maximum storm tide due to hurricanes and other tropical storms, Mon. Weather Rev., 85, 113–116, 1957.

Deo, M. C. and Sridhar Naidu, C.: Real time wave forecasting using neural networks, Ocean Eng., 26, 191–203, 1999.

Doong, D.-J., Chuang, L. Z.-H., Wu, L.-C., Fan, Y.-M., Kao, C. C., and Wang, J.-H.: Development of an operational coastal flooding early warning system, Nat. Hazards Earth Syst. Sci., 12, 379–390, doi:10.5194/nhess-12-379-2012, 2012.

Grubert, J. P.: Prediction of estuarine instabilities with artificial neural network, J. Comput. Civil Eng., 9, 266–274, 1995.

Harper, B. A. and Sobey, R. J.: Open-boundary conditions for open-coast hurricane storm surge, Coastal Eng. Japan, 7, 41–60, 1983.

Haykin, S.: Neural Networks: A Comprehensive Foundation, Pearson Education, Inc., 1999.

Horikawa, K.: Coastal Engineering, Tokyo University Press, 1978.

Hsu, T. W., Liao, J. M., and Lee, Z. S.: Prediction of storm surge at northestern coast of Taiwan by finite element method, J. Chinese Institute Civil Hydraulic Eng., 11, 849–857, 1999.

Hwang, R. R. and Yao, C. C.: A semi-implicit numerical model for storm surges, J. Chin. Institute Eng., 10, 463–472, 1987.

Kawahara, M., Nakazawa, S., Ohmori, S., and Tagaki, T.: Two-step explicit finite element method for storm surge propagation analysis, Int. J. Numer. Meth. Eng., 15, 1129–1148, 1980.

Lee, T. L., Tsai, C. P., Jeng, D. S., and Shieh, R. J.: Neural network for the prediction and supplement of tidal record in Taichung Harbor, Taiwan. Adv. Eng. Software, 33, 329–338, 2002.

Lin, G. F. and Chen, G. R.: An improved neural network approach to the determination of aquifer parameters, J. Hydrol., 316, 281–289, 2006.

Murty, T. S.: Storm surges: Meteorological ocean tides, Canadian Bulletin of Fisheries and Aquatic Science 212, Dept. Fisheries and Oc., Canada, 1984.

Rumelhart, D. E., Hinton, G. E., and Williams, R. J.: Learning representations by back-propagating errors, Nature, 323, 533–536, 1986.

Sztobryn, M.: Forecast of storm surge by means of artificial neural network, J. Sea Res., 49, 317–322, 2003.

Tsai, C. P. and Lee, T. L.: Back-propagation neural network in tidal-level forecasting, J. Waterway Port Coast. Ocean Eng. ASCE, 125, 195–202, 1999.

Tsai, C. P., Lin, C., and Shen, J. N.: Neural network for wave forecasting among multi-stations, Ocean Eng., 29, 1683–1695, 2002.

Tsai, C. P., Lee, T. L., Yang, T. J., and Hsu, Y. J.: Back-propagation neural networks for prediction of storm surge, Proceedings of the Eighth International Conference on the Application of Artificial Intelligence to Civil, Structural and Environmental Eng., Paper (45), Civil-comp Press, UK, 2005.

Tsai, H. S., Chen, M. J., and Yen, C. L.: Study of typhoon surge deviation on the mouth of Tanshui River, Proceedings of the 11th Conference on Hydrogenic Engineering, Taipei, Taiwan, C115–C120, 2000.

Tseng, C. M., Jan, C. D., Wang, J. S., and Wang, C. M.: Application of artificial neural networks in typhoon surge forecasting, Ocean Eng., 34, 1757–1768, 2007.

Walton, R. and Christensen, B. A.: Friction factors in storm surges over inland areas, J. Waterway Port Coast. Ocean Division ASCE, 106, 261–271, 1980.

Westerink, J. J., Luettich, R. A., Baptista, A. M., Scheffner, N. W., and Farrar, P.: Tide and storm surge predictions using a finite element model, J. Hrdraulic Eng. ASCE, 118, 1373–1390, 1992.

Xu, S., Huang, W., Zhang, G., Gao, F., and Li, X.: Integrating Monte Carlo and hydrodynamic models for estimating extreme water levels by storm surge in Colombo, Sri Lanka, Nat. Hazards, 71, 703–721, 2014.

Yen, G. T. and Chou, F. K.: Moving boundary numerical surge model, J. Waterway Port Coast. Ocean Div. ASCE, 105, 247–263, 1979.